ACS Medicinal Chemistry Letters

Letter

pubs.acs.org/acsmedchemlett

Potent Targeting of the STAT3 Protein in Brain Cancer Stem Cells: A Promising Route for Treating Glioblastoma

Sina Haftchenary,[†,#] H. Artee Luchman,[‡,#] Andriana O. Jouk,[†] Anthony J. Veloso,[§] Brent D. G. Page,[†] Xin Ran Cheng,[§] Sean S. Dawson,[†] Natalie Grinshtein,[∥] Vijay M. Shahani,[†] Kagan Kerman,[§] David R. Kaplan,[∥] Carly Griffin,[⊥] Ahmed M. Aman,[⊥] Rima Al-awar,[⊥] Samuel Weiss,[‡] and Patrick T. Gunning*[,†]

[†]Department of Chemical and Physical Sciences, University of Toronto at Mississauga, Mississauga, ON L5L 1C6, Canada

[‡]Hotchkiss Brain Institute and Department of Cell Biology and Anatomy, University of Calgary, Calgary, AB T2N 1N4, Canada

[§]Department of Chemistry, University of Toronto at Scarborough, Toronto, ON M1C 1A4, Canada

[∥]Cell Biology Program and James Burrel Laboratories at the Hospital for Sick Children, Toronto, ON M5G 1X8, Canada

[⊥]Drug Discovery Program, Ontario Institute for Cancer Research, Toronto, ON M5G 0A3, Canada

Supporting Information

ABSTRACT: The *STAT3* gene is abnormally active in glioblastoma (GBM) and is a critically important mediator of tumor growth and therapeutic resistance in GBM. Thus, for poorly treated brain cancers such as gliomas, astrocytomas, and glioblastomas, which harbor constitutively activated STAT3, a STAT3-targeting therapeutic will be of significant importance. Herein, we report a most potent, small molecule, nonphosphorylated STAT3 inhibitor, **31 (SH-4-54)** that strongly binds to STAT3 protein (K_D = 300 nM). Inhibitor **31** potently kills glioblastoma brain cancer stem cells (BTSCs) and effectively suppresses STAT3 phosphorylation and its downstream transcriptional targets at low nM concentrations. Moreover, in vivo, **31** exhibited blood−brain barrier (BBB) permeability, potently suppressed glioma tumor growth, and inhibited pSTAT3 in vivo. This work, for the first time, demonstrates the power of STAT3 inhibitors for the treatment of BTSCs and validates the therapeutic efficacy of a STAT3 inhibitor for GBM clinical application.

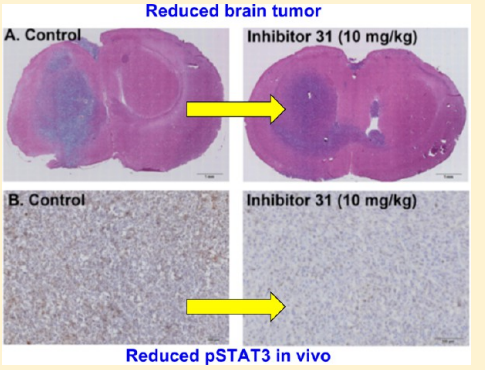

KEYWORDS: *STAT3, BTSCs, glioblastoma, small-molecule inhibitor, antitumor cell effects*

Glioblastoma (GBM) is considered the most aggressive and lethal of brain cancers, with a median survival after treatment of approximately 15 months; shockingly, these modest results can only be achieved in the relatively young, otherwise healthy patients.[1] Moreover, GBM is neither preventable, nor detectable at a stage when early treatment might be more effective. Furthermore, despite intensive research, major improvements in overall survival have remained elusive.

Brain tumors have been demonstrated to contain rare subpopulations of brain tumor stem cells (BTSCs), which possess the cardinal stem cell properties of clonogenic self-renewal, multipotency, and tumorigenicity.[2] The extensive self-renewal and proliferative capacity of BTSCs coupled with their insensitivity to conventional radio- and chemotherapies[3,4] suggest that they are integral to the growth and post-treatment recurrence of GBM. As such, BTSCs represent a reservoir of disease that require novel therapeutic approaches to eliminate in order to improve the outcome of GBM. Recently, Carro et al.[5] demonstrated that the signal transducer and activator of transcription 3 (STAT3) gene is abnormally active in GBM, and is a critically important mediator of tumor growth and therapeutic resistance in GBM. Poorly treated brain cancers such as gliomas, astrocytomas, and glioblastomas harbor constitutively activated STAT3. In addition, a growing body of recent evidence gathered using a variety of different small molecules that indirectly inhibit STAT3 by targeting upstream molecules such as the JAK family members[6] strongly suggest that STAT3 signaling is crucial for the survival and proliferation of BTSCs and GBM both in vitro and in vivo.[7] However, because of their broad targeting nature, these drugs have limited translational potential due to numerous side effects. Hence, drugs with the ability to more specifically block STAT3 activity may provide effective treatment of GBM.

Briefly, STAT3 is a member of the STAT family of transcription factor proteins. STAT3 is activated through phosphorylation of tyrosine 705 (Y705) that initiates complexation of two phosphorylated STAT3 monomers (pSTAT3).

Received: August 13, 2013
Accepted: September 8, 2013

   dx.doi.org/10.1021/ml4003138 | *ACS Med. Chem. Lett.* XXXX, XXX, XXX−XXX

pSTAT3 homodimers are mediated through reciprocal STAT3 Src Homology 2 (SH2) domain-pY705 STAT3 interactions. pSTAT3:pSTAT3 homodimers translocate to the nucleus and bind DNA, promoting STAT3 target gene transcription.[8] Targeting STAT3 has been achieved with dominant negative constructs, oligonucleotides,[9] or, most commonly, phosphopeptidic agents that mimic the native pY705 containing binding sequence[10−13] or non-native STAT3-binding sequences.[14,15] Unfortunately, these inhibitors, possessing pTyr-like groups, are poorly cell permeable and rapidly metabolized in vivo, which has limited their use in the clinic. To circumvent these problems, our group has developed novel small molecule STAT3 inhibitors not containing a phosphate ester.[16,17] Using structure-based design, targeting the pTyr-SH2 domain interactions, salicylic acid-based inhibitors have been identified that block STAT3 dimerization and DNA-binding, namely, **BP-1-102** (**1**, Figure 1). **BP-1-102** potently suppresses cell

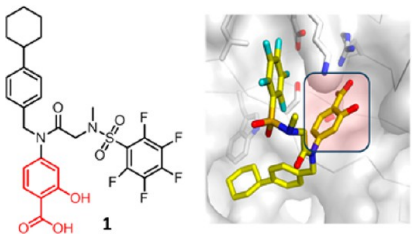

Figure 1. In silico docking images of inhibitor **1**.

proliferation, migration, invasion, and motility. It showed little or no effect on phosphorylation of Jak-1/2, Shc, Src, or Akt. **BP-1-102** exhibited potent antitumor effects in in vivo xenograft models of lung and breast cancer. Western blots of tumors showed repression in pSTAT3 in a dose-dependent manner.[18−20] We hypothesized that since the STAT3 pathway is a key oncogenic driver in brain tumor stem cells, direct inhibition of STAT3 would provide a targeted route for managing GBM. In this study, we have optimized **1** to be more potent, possess reduced pharmacokinetic labilities and effectively penetrate the blood brain barrier (BBB).

A library of **BP-1-102** analogues possessing both prodrugs and potential bioisosteres, as well as salicylic acid mimics, were prepared (Table 1). For improving cell and BBB permeability, prodrugs were synthesized to conceal the carboxylate functionality. In this family, alkyl (**21** and **22**), acetoxymethyl (AOM) (**23**), pivaloyloxymethyl (POM) (**24**), and the acetylated prodrug (**19**) were prepared to enhance cell penetration. We prepared a nonhydrolyzable phosphonate, **18**, as well as its prodrug, **16**. In addition, the relative ring positions of the hydroxy- and carboxylate groups of the salicylic acid were inversed (**34**), the hydroxyl substituent replaced with a fluoride (**33**) or removed entirely and replaced with a hydrogen atom (**31**). The fluorinated analogue, **33**, was prepared to reduce the charge on the carboxylate and preclude phase II glucoronidation of the phenol. To investigate the salicylic acid's role in binding STAT3, an *N*-hydroxyl amino (**32**), sulfonamide (**10**−**13**), sulfonamine (**14**), tetrazole (**29** and **35**) and *N*-hydoxy-oxamic acid (**25**) derivatives were prepared. As negative controls, we prepared **10**, **11**, and **30**, which possessed hydrophobic naphthyl or benzene groups in place of the salicylic acid.

First, the library was screened for biological activity against GBM BTSC line 30M, derived from a GBM patient. Cell

Table 1. Focused Library of Inhibitors Consisting of Prodrugs and Bioisosteres of the Salicylic Acid Functionality

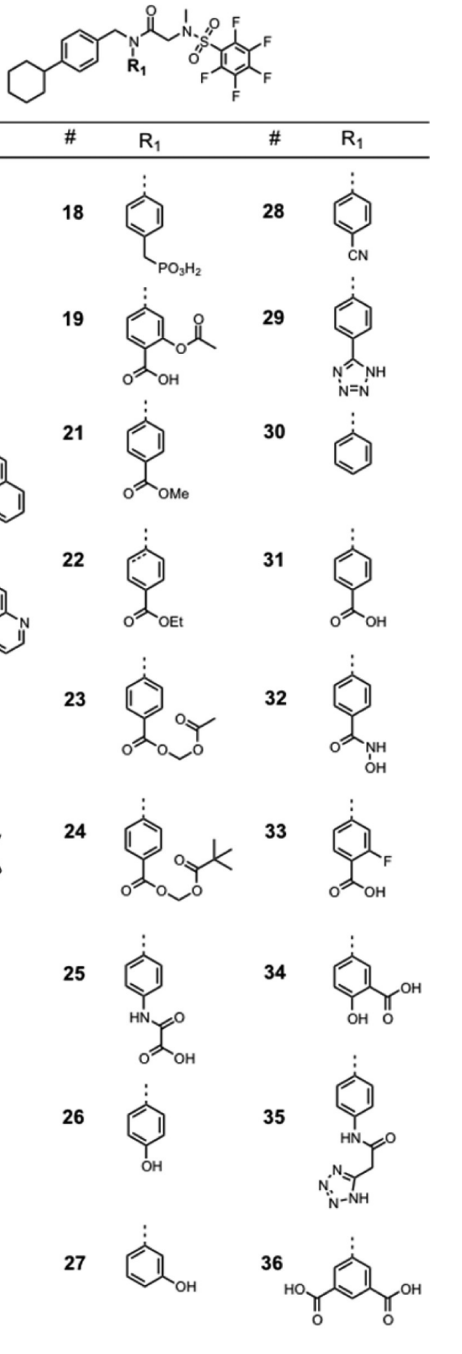

viability following drug treatment was assessed after 72 h using an alamarBlue assay.[6,21] IC_{50} values were derived and compared to **BP-1-102**. Consistent with previous findings, **BP-1-102** exhibited low micromolar activity (Figure 2A). More encouragingly, we identified a number of more potent inhibitors exhibiting low nanomolar IC_{50} values. Lead compounds were then evaluated against a panel of BTSCs, 25EF, 67EF, 73E, 84EF, and 127EF, which are molecularly heterogeneous human GBM BTSCs (Figure 2B). Compounds displayed IC_{50} values ranging from 0.1 to 3.8 μM in comparison to **BP-1-102**, which displayed values above 2−5 μM (BTSC 30M). Compounds SH-05-19 (**19**), SH-04-54 (**31**), SH-05-07 (**32**), and SH-05-23 (**33**) showed potent activity, with IC_{50}s

dx.doi.org/10.1021/ml4003138 | ACS Med. Chem. Lett. XXXX, XXX, XXX−XXX

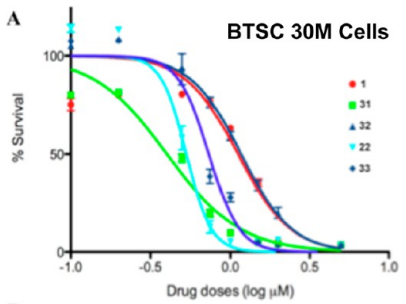

B

IC50 (nM) against BTSCs	19 (SH-05-19)	31 (SH-04-54)	32 (SH-05-07)	33 (SH-05-23)
25EF	1145 ± 162.6	234 ± 73.4	1120.5 ± 301.9	592 ± 195.2
67EF	435.5 ± 176.1	106 ± 19.8	214.5 ± 36.1	214 ± 93.4
73EF	1075 ± 247.5	162 ± 59.4	863.5 ± 443.4	438 ± 107.5
84EF	332 ± 16.9	102 ± 2.8	295 ± 35.4	202.5 ± 17.7
127EF	272.5 ± 24.8	66 ± 33.9	195.5 ± 20.5	90 ± 14.2

Figure 2. (A) Comparison of **BP-1-102** (**1**) against the top four from the new library in BTSC30M; (B) IC_{50} values of top four inhibitors against BTSCs 25EF, 67EF, 73E, 84EF, and 127EF.

ranging from 66−1145 nM. However, **31**, equipped with a benzoic acid substituent, exhibited higher potency against a larger number of BTSCs and represents a most potent inhibitor of BTSCs (Supporting Information). Inhibitors were next assessed against normal human fetal astrocytes (healthy cells) at concentrations of up to 5 μM. As shown in Figure 3A, **19**, **31**, and **32** showed minimal toxicity at 5 μM, identifying a clear therapeutic window for these agents.

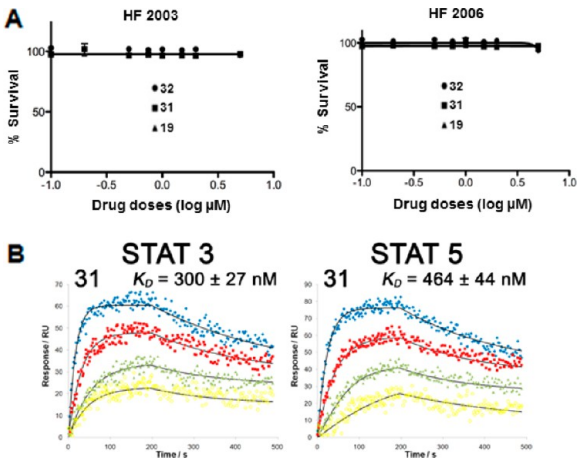

Figure 3. (A) Top three hits showed minimal cytotoxicity against normal human fetal astrocyte cells; (B) SPR curves displaying the binding affinity of the best hit, **31**, to STAT 3/5 proteins. Studies were done at multiple concentrations (5.000, 1.667, 0.556, and 0.185 μM).

Next, to determine kinetic association and dissociation rate constants (k_{on} and k_{off}), surface plasmon resonance (SPR) binding experiments were performed using a ProteOn XPR36 (Biorad) with full length His-tagged STAT3 protein immobilized on THE sensor chips. Promisingly, lead agents exhibited nanomolar binding potencies with **31**, the most potent, exhibiting a K_D (k_{off}/k_{on}) of 300 ± 27 nM (Figure 3B). Thus, **31** represents a most potent, nonphosphorylated, small molecule STAT3 inhibitor. While phosphopeptides have been reported to bind to STAT3 with nanomolar potency, these agents have not shown in vivo efficacy.[22] Comparative SPR analysis against STAT5, an analogous member of the STAT family proteins, showed modest selectivity (K_D = 464 nM). Since the BTSCs evaluated do not harbor hyperactivated STAT5 (Supporting Information), we cannot attribute the observed activity to anti-STAT5 activity.

Next, to examine phosphopeptide:STAT3 SH2 domain disruption, compounds were subjected to a fluorescence polarization (FP) assay.[23,24] As expected, prodrugs **15**−**16** and **19**−**24** displayed no disruptive potency. Inhibitors **31**, **32**, and **33** showed good inhibitory potency, disrupting STAT3:-phosphopeptide interactions with K_is ranging from 10 to 30 μM. Encouragingly, **33**, **31**, and **32** were selective for STAT3 over STAT1, a tumor suppressor protein (2-, 4-, and >10-fold selectivity for STAT3, respectively (Supporting Information). Concerned that binding affinity was due to hydrophobic aggregation, we tested **30**, which lacks the salicylic acid, and found that it had no binding affinity for the STAT3 protein (Supporting Information), thus confirming the requirement for the carboxylate for **31**'s binding potency.

Next, **19**-, **31**-, and **32**-mediated inhibition of cellular levels of activated pSTAT3 activity were determined using Western Blot analysis for phosphorylated STAT3 (pY705 and pS727) as well as for downstream target genes, Bcl-xL and Cyclin D1 (Figure 4A). Inhibitors exhibited concentration-dependent and potent

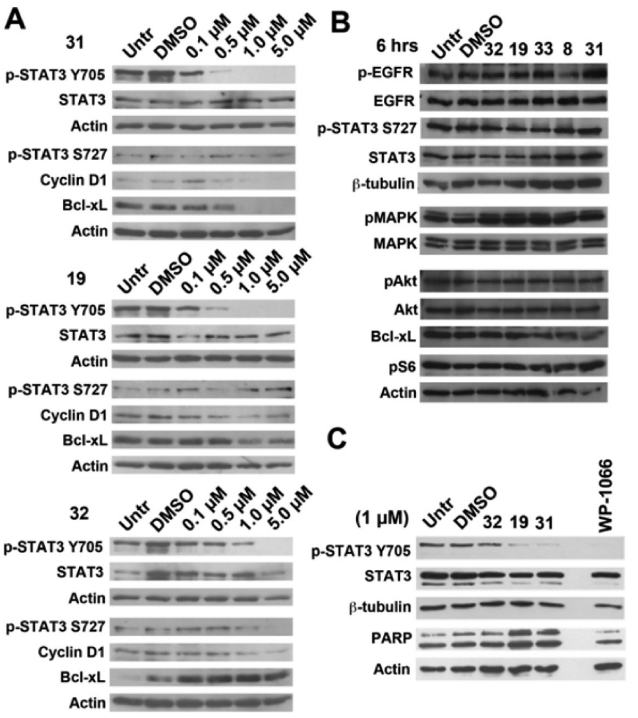

Figure 4. (A) Compounds effectively attenuate pSTAT3 Y705 with no effect on pSTAT3 Ser727; (B) exhibit no off-target effects in various signaling pathways; (C) Western blot analysis of top agents in comparison against Jak2 inhibitor, WP1066.

(nM) suppression of pSTAT3 (Y705) with no effect on the total STAT3 levels or on pSTAT3 (S727). Of note, blockade of the STAT3 SH2 domain should not inhibit S727 phosphorylation, suggesting that our molecules were binding the SH2 domain. Further Western analysis for inhibition of upstream kinase targets including, JaK2, Src, (Supporting Information), Akt, MAPK, and EGFR showed no off-target effects (Figure 4B). Most encouragingly, dose-dependent decreases in pSTAT3 levels were observed as well as potent inhibition of downstream targets involved in cell growth and survival (Cyclin D1 and Bcl-xL). Notably, **31** exhibited concentration-depend-

dx.doi.org/10.1021/ml4003138 | ACS Med. Chem. Lett. XXXX, XXX, XXX−XXX

ent decreases in pSTAT3 levels that correlated well with observed cytotoxicity and downstream target suppression. Treatment with **31** (500 nM) silenced pSTAT3 signaling in 147EF cells. Inhibitors **19** and **32**, while less potent, exhibited nanomolar inhibition of pSTAT3.

To evaluate potential off-target effects, **19**, **31**, and **32** were screened in vitro for activity against cancer related kinases, c-Src, ERK1, Akt, JaK1, and JaK2 at 5 μM (Supporting Information). Inhibitors exhibited moderate to negligible activity against the kinases tested. Compounds showed negligible inhibition of Akt1, Erk1, and JaK1, while only exhibiting modest inhibition of JaK2, c-Src, and JaK2 (~50% inhibition at 5 μM). Since the concentration of inhibitor required to elicit effective kinase inhibition was 15-fold higher than the IC_{50} values in BTSCs, we concluded that activity was not a result of JaK kinase inhibition.

To comprehensively investigate potential off-target effects, **31** was subjected to a kinome screen (101 diverse kinases, DiscoveRx) as well as a protein and receptor screen (21 biologically important G protein-coupled receptors (GPCRs)). For kinome screening, ultrasensitive quantitative PCR (qPCR) was used to measure levels of immobilized kinases after treatment with **31**.[12] The GPCR screening employed the PathHunter β-arrestin assay platform (DiscoveRx) to evaluate **31**. Encouragingly, **31** showed no off-target activity against any of the 21 GPCRs tested (500 nM). Moreover, in the kinome screen (500 nM), **31** showed negligible effects against SH2 (JaK1/2) and SH3 (Fes, Fer, and Fyn) containing kinases with the exception of 35% inhibition of PDGFRB, a kinase implicated in glioblastoma.[25] Concerned that **31** may act on PDGFRB to inhibit STAT3 activity, we conducted Western Blot analysis for activated PDGFRB in BTSCs evaluated as well as to determine the IC_{50} value of **31** against PDGFRB in vitro. Encouragingly, we found that PDGFRB activity was not present in any of the BTSCs examined (Supporting Information), and furthermore, as assessed by an enzymatic assay, **31** did not inhibit PDGFRB at concentrations of 10 μM (Supporting Information). Thus, to the best of our knowledge **31** directly inhibits STAT3.

Next, we compared **31** to a potent JaK2 inhibitor, WP1066, in 73 M BTSCs (Figure 4C).[6] Western blot analyses showed equipotent suppression of pSTAT3 at 1 μM. In a cytotoxicity assay, **31** was found to be more potent (30 M, **31** IC_{50} = 0.43 μM, cf. WP1066 IC_{50} = 1.8 μM, and in 73 M, **31** IC_{50} = 1.03 μM, cf. WP1066 IC_{50} = 2.1 μM (Supporting Information). Notably, **31** does not inhibit JaKs at therapeutic doses and appears to function through direct STAT3 inhibition.[26,27] In addition, Western blot analysis of **31** vs **1**, where comparative effects against pSTAT3 and pAkt were measured, as well as induced apoptosis as measured by cleaved PARP, demonstrated the superiority of **31** (Supporting Information).

To evaluate BBB penetration in vivo, **31** and **32** were given to three mice at 10 mg/kg and 25 mg/kg dosing (analogous to **BP-1-102** in vivo dosing) via intraperitoneal injection, and blood was collected at two time points (30 and 300 min). Brain was also collected from one mouse at each dose and concentrations of **31** and **32** determined by LCMS. We found that after 30 min at 10 mg/kg, compound **31** was found at a concentration of 313 ± 8 nM (Supporting Information). Following these studies, three mice per group were dosed for five consecutive days with 10 mg/kg. Blood was collected at 30 and 300 min post the last dose, and brain was collected from all animals at the 300 min time-point. Then, 313 ± 8 nM of **31** was detected in the brains of treated animals (Supporting Information). Encouragingly, these studies demonstrated that therapeutic doses of **31** could be achieved in vivo at values similar to the in vitro IC_{50}s demonstrating efficacy against BTSCs.

Next, to evaluate **31** in vivo, NOD-SCID mice were orthoptopically xenografted with 10^5 BT73 glioma cells. On the basis of the results for the above in vivo PK/PD and five-day maximum tolerated dose study, animals were dosed with 10 mg/kg **31**, in order to achieve drug accumulation in the brains of the NOD-SCID mice at doses similar to in vitro IC_{50}s (Supporting Information). Therefore, starting on day 7, mice were given 10 doses of 10 mg/kg intraperitoneal injection of **31** or vehicle control on 4 days on/3 days off schedule. Animals were sacrificed 2 h after the last dose and brain tumors extracted and immunohistochemistry performed for pSTAT3, Ki67 (proliferation), and TUNEL (apoptosis). Analysis of tumors showed decreased tumor cells in **31** treated mice using Hematoxylin/Eosin staining (Figure 5A). Significantly, **31** decreased pSTAT3 expression in tumor cells of treated mice (Figure 5B). Furthermore, **31** appears to decrease proliferation (Figure 5C) and increase apoptosis (Figure 5D) of treated tumors. Thus, in vivo studies strongly suggest in vivo potency and on-target anti-STAT3 activity.

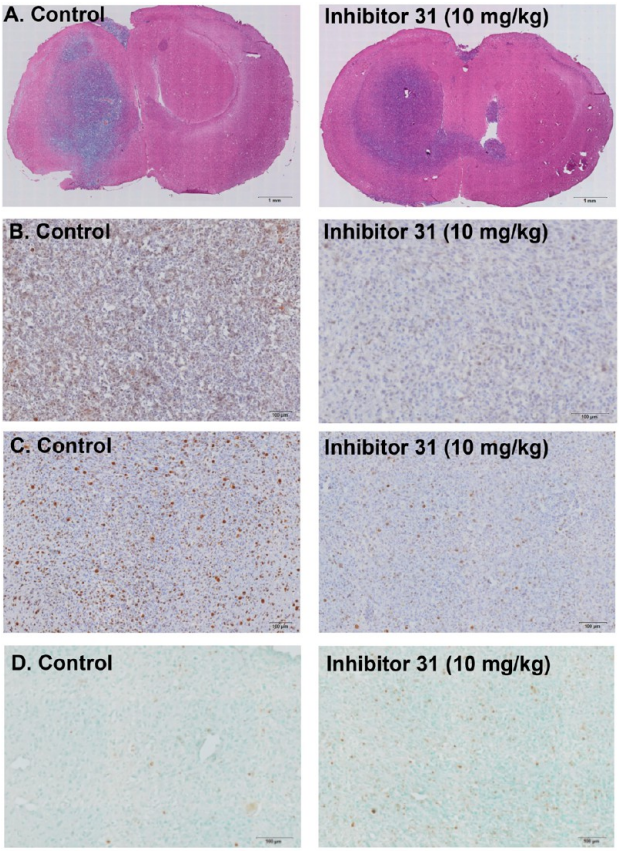

Figure 5. (A) Hematoxylin/Eosin staining: hypercellular tumor dense areas staining blue with hematoxylin. The images display brain tumor suppression and a normal brain morphology for the mice treated with **31**; (B) decreased pSTAT3 in mice orthotopically xenografted with BT73 and treated with **31**; (C) decreased expression of proliferation marker Ki67 in mice treated with **31**; (D) increased apoptosis (TUNEL staining) in mice treated with **31**.

dx.doi.org/10.1021/ml4003138 | ACS Med. Chem. Lett. XXXX, XXX, XXX−XXX

In summary, to the best of our knowledge, we have identified a most potent, nonphosphorylated direct binding STAT3 inhibitor, **31** (**SH-4-54**). Compound **31** exhibited nanomolar K_D values for STAT3, showed unprecedented cytotoxicity in human BTSCs, displayed no toxicity in human fetal astrocytes, potently suppressed pSTAT3 with nanomolar IC_{50}s, inhibited STAT3's downstream targets, and showed no discernible off-target effects at therapeutic doses. Moreover, in vivo, **31** exhibits BBB permeability, potently suppresses glioma tumor growth, and inhibits pSTAT3 in vivo. This work, for the first time, demonstrates the power of STAT3 inhibitors for the treatment of BTSCs and validates the therapeutic efficacy of a STAT3 inhibitor for GBM clinical application.

■ ASSOCIATED CONTENT

Ⓢ Supporting Information

Information on synthesis, characterization, detailed results, and experimental procedures for SPR, Cytotoxicity, BBB permeability, and in vivo assays. This material is available free of charge via the Internet at http://pubs.acs.org.

■ AUTHOR INFORMATION

Corresponding Author

*(S.T.G.) E-mail: patrick.gunning@utoronto.ca.

Author Contributions

#S.H. and H.A.L. contributed equally to this work.

Funding

Financial support was provided by Boehringer Ingelheim Canada (to P.T.G.), Stem Cell Network (to S.W. and P.T.G.), NSERC Discovery Grant (to P.T.G. and K.K.), NSERC Graduate Scholarship (S.H. and B.D.G.P.), and Ontario Graduate Scholarship (to V.M.S.).

Notes

The authors declare no competing financial interest.

■ REFERENCES

(1) Stupp, T.; Mason, W. P.; Van den Bent, M. J.; Weller, M.; Fisher, B.; Taphoorn, M. J.; Belanger, K.; Brandes, A. A.; Marosi, C.; Bogdahn, U.; Curschmann, J.; Janzer, R. C.; Ludwin, S. K.; Gorlia, T.; Allgeier, A. L.; Lacombe, D.; Cairncross, J. G.; Eisenhauer, E.; Mirimanoff, R. O. Radiotherapy plus concomitant and adjuvant temozolomide for glioblastoma. *New Engl. J. Med.* **2005**, *352*, 987−96.

(2) Yuan, S. H.; Martin, J.; Elia, J.; Flippin, J.; Paramban, R. I.; Hefferan, M. P.; Vidal, J. G.; Mu, Y.; Killian, R. L.; Israel, M. A.; Emre, N.; Marsala, S.; Marsala, M.; Gage, F. H.; Goldstein, L. S.; Carson, C. T. Cell-surface marker signatures for the isolation of neural stem cells, glia and neurons derived from human pluripotent stem cells. *PLoS One* **2011**, *6*, e17540.

(3) Bleau, A. M.; Hambardzumyan, D.; Ozawa, T.; Fomchenko, E. I.; Huse, J. T.; Brennan, C. W.; Holland, E. C. PTEN/PI3K/Akt pathway regulates the side population phenotype and ABCG2 activity in glioma tumor stem-like cells. *Cell Stem Cell* **2009**, *3*, 226−35.

(4) Salmaggi, A.; Boiardi, A.; Gelati, M.; Russo, A.; Calatozzolo, C.; Ciusani, E.; Sciacca, F. L.; Ottolina, A.; Parati, E. A.; La Porta, C.; Alessandri, G.; Marras, C.; Croci, D.; De Rossi, M. Glioblastoma-derived tumorospheres identify a population of tumor stem-like cells with angiogenic potential and enhanced multidrug resistance phenotype. *Glia* **2006**, *54*, 850−860.

(5) Carro, M. S.; Lim, W. K.; Alvarez, M. J.; Bollo, R. J.; Zhao, X.; Snyder, E. Y.; Sulman, E. P.; Anne, S. L.; Doetsch, F.; Colman, H.; Lasorella, A.; Aldape, K.; Califano, A.; Iavarone, A. The transcriptional network for mesenchymal transformation of brain tumours. *Nature* **2010**, *463*, 318−325.

(6) Stechishin, O. D.; Luchman, H. A.; Ruan, Y.; Blough, M. D.; Nguyen, S. A.; Kelly, J. J.; Cairncross, J. G.; Weiss, S. On-target JAK2/STAT3 inhibition slows disease progression in orthotopic xenografts of human glioblastoma brain tumor stem cells. *Neuro-Oncology* **2013**, *15*, 198−207.

(7) Villalva, C.; Martin-Lannerée, S.; Cortes, U.; Dkhissi, F.; Wager, M.; Le Corf, A.; Tourani, J. M.; Dusanter-Fourt, I.; Turhan, A. G.; Karayan-Tapon, L. STAT3 is essential for the maintenance of neurosphere-initiating tumor cells in patients with glioblastomas: A potential for targeted therapy? *Int. J. Cancer* **2011**, *128*, 826−838.

(8) Haftchenary, S.; Avadisian, M.; Gunning, P. T. Towards the development of small molecule inhibitors of Stat3 dimerization. *Anti-Cancer Drugs* **2011**, *22*, 115−127.

(9) Leong, P. L.; Andrews, G. A.; Johnson, D. E.; Dyer, K. F.; Sichuan, X.; Jeffrey, C. M.; Robbins, P. D.; Gadiparthi, S.; Burke, N. A.; Watkins, S. F.; Grandis, J. R. Targeted inhibition of Stat3 with a decoy oligonucleotide abrogates head and neck cancer cell growth. *Proc. Natl. Acad. Sci. U.S.A.* **2003**, *7*, 4138−4143.

(10) Chen, X.; Vinkemeier, U.; Zhao, Y.; Jeruzalmi, D.; Darnell, J. E.; Kuriyan, J. Crystal structure of a tyrosine phosphorylated STAT-1 dimer bound to DNA. *Cell* **1998**, *93*, 827−839.

(11) Xi, S.; Gooding, W. E.; Grandis, J. R. In vivo antitumor efficacy of STAT3 blockade using a transcription factor decoy approach: Implications for cancer therapy. *Oncogene* **2005**, *24*, 970−979.

(12) Stahl, N.; Farruggella, T. J.; Boulton, T. G.; Zhong, Z.; Darnell, J. E.; Yancopoulos, G. D. Choice of STATs and other substrates specified by modular tyrosine-based motifs in cytokine receptors. *Science* **1995**, *267*, 1349−1353.

(13) Shahani, V. M.; Yue, P.; Fletcher, S.; Sharmeen, S.; Sukhai, M. A.; Luu, D. P.; Zhang, X.; Sun, H.; Zhao, W.; Schimmer, A. D.; Turkson, J.; Gunning, P. T. Design, Synthesis and in vitro characterization of novel hybrid peptidomimetic inhibitors of STAT3 protein. *Bioorg. Med. Chem.* **2011**, *19*, 1823−1838.

(14) Chen, J.; Bai, L.; Bernard, D.; Nikolovska-Coleska, Z.; Gomez, C.; Zhang, J.; Yi, H.; Wang, S. Structure-based design of conformationally constrained, cell-permeable STAT3 inhibitors. *ACS Med. Chem. Lett.* **2010**, *1*, 85−89.

(15) Mao, X.; Ren, Z.; Parker, G. N.; Sondermann, H.; Pastorello, M. A.; Wang, W.; McMurray, J. S.; Demeler, B.; Darnell, J. E., Jr.; Chen, X. Structural bases of unphosphorylated STAT1 association and receptor binding. *Mol. Cell* **2005**, *17*, 761−771.

(16) Fletcher, S.; Singh, J.; Zhang, X.; Yue, P.; Page, B. D. G.; Sharmeen, S.; Shahani, V. M.; Zhao, W.; Schimmer, A. D.; Turkson, J.; Gunning, P. T. Disruption of transcriptionally active Stat3 dimers with non-phosphorylated, salicylic acid-based small molecules: Potent in vitro and tumor cell activities. *ChemBioChem* **2009**, *10*, 1959−1964.

(17) Page, B. D. G.; Fletcher, S.; Yue, P.; Li, Z.; Zhang, X.; Sharmeen, S.; Datti, A.; Wrana, J. L.; Trudel, S.; Schimmer, A. D.; Turkson, J.; Gunning, P. T. Identification of a nonphosphorylated, cell permeable, small molecule ligand for the Stat3 SH2 domain. *Bioorg. Med. Chem.* **2011**, *21*, 5605−5609.

(18) Fletcher, S.; Page, B. D. G.; Zhang, X.; Yue, P.; Li, Z. H.; Sharmeen, S.; Singh, J.; Zhao, W.; Schimmer, A. D.; Trudel, S.; Turkson, J.; Gunning, P. T. Antagonism of the Stat3−Stat3 protein dimer with salicylic acid-based small molecules. *ChemMedChem* **2011**, *6*, 1459−1470.

(19) Zhang, X.; Yue, P.; Page, B. D. G.; Lia, T.; Zhao, W.; Namanja, A. T.; Paladino, D.; Zhaoa, J.; Chen, Y.; Gunning, P. T.; Turkson, J. An orally-bioavailable small-molecule Stat3 inhibitor regresses human breast and lung cancer xenografts. *Proc. Natl. Acad. Sci.* **2012**, *33*, 2450−2456.

(20) Page, B. D. G.; Khoury, H.; Laister, R. C.; Fletcher, S.; Vellozo, M.; Manzoli, A.; Yue, P.; Turkson, J.; Minden, M. D.; Gunning, P. T. Small molecule STAT5-SH2 domain inhibitors exhibit potent anti-leukemia activity. *J. Med. Chem.* **2012**, *55*, 1046−1055.

(21) Kelly, J. J.; Stechishin, O.; Chojnacki, A.; Lun, X.; Sun, B.; Senger, D. L.; Forsyth, P.; Auer, R. N.; Dunn, J. F.; Cairncross, J. G.; Parney, I. F.; Weiss, S. Proliferation of human glioblastoma stem cells occurs independently of exogenous mitogens. *Stem Cells* **2009**, *27*, 1722−1733.

401 (22) Coleman, D. R.; Ren, Z.; Mandal, P. K.; Cameron, A. G.; Dyer,
402 G. A.; Muranjan, S.; Campbell, M.; Chen, X.; McMurray, J. S.
403 Investigation of the binding determinants of phosphopeptides targeted
404 to the SRC homology 2 domain of the signal transducer and activator
405 of transcription 3. Development of a high-affinity peptide inhibitor. *J.*
406 *Med. Chem.* **2005**, *48*, 6661−6670.
407 (23) Schust, J.; Berg, T. A high-throughput fluorescence polarization
408 assay for STAT3. *Anal. Biochem.* **2004**, *330*, 114−118.
409 (24) Wu, P.; Brasseur, M.; Schindler, U. A high-throughput STAT
410 binding assay using fluorescence polarization. *Anal. Biochem.* **1997**,
411 *249*, 29−36.
412 (25) Verkaar, F.; Van Rosmalen, J. W.; Blomenröhr, M.; Van
413 Koppen, C. J.; Blankesteijn, W. M.; Smits, J. F.; Zaman, G. J. G
414 protein-independent cell-based assays for drug discovery on seven-
415 transmembrane receptors. *Biotechnol. Annu. Rev.* **2008**, *14*, 253−274.
416 (26) McFarland, B. C.; Ma, J. Y.; Langford, C. P.; Gillespie, G. Y.; Yu,
417 H.; Zheng, Y.; Nozell, S. E.; Huszar, D.; Benveniste, E. N. Therapeutic
418 potential of AZD1480 for the treatment of human glioblastoma. *Mol.*
419 *Cancer Ther.* **2011**, *12*, 2384−2393.
420 (27) Tefferi, A. JAK inhibitors for myeloproliferative neoplasms:
421 clarifying facts from myths. *Blood* **2012**, *119*, 2721−27.